

Statistical Limitations of TDC Density Tests

Matthew W. Fishburn, *Student Member, IEEE*, and Edoardo Charbon, *Senior Member, IEEE*

Time-to-digital converters (TDCs) occur in many realms of high-energy physics, such as time-of-flight positron emission tomography (TOF PET)[1]. Density tests[2] are often used to characterize the non-uniformity of TDCs. Such tests require a uniform time interval generator, often realized by a probabilistic exponential source, such as a single-photon avalanche diode (SPAD), and a known time reference. However, if the exponential source's event rate is too large, static distortions will occur in the measured INL. Additionally, the correlated shot noise created by the probabilistic source will introduce some uncertainty into measurements of the differential non-linearity (DNL) and integral non-linearity (INL). This paper will discuss these two unwanted effects, and present measurements showing that the analysis is correct.

Let a TDC have its start input connected to a probabilistic exponential source with rate parameter λ , and the stop input be connected to a reference clock with period m (with units of seconds) that is smaller than the TDC's range. Let C be the number of TDC codes corresponding to range m , s_z the number of samples of code z during a density test with N trials, and d_z the actual value of the DNL of code z . The measured DNL \hat{d}_z is $s_z/(N/c) - 1$. The s_z variables are governed by a binomial process, with probability $(d_z + 1)/C$ per-trial of code z being sampled, giving

$$\text{var}(s_z) = N \frac{(d_z + 1)(C - d_z - 1)}{C^2}, \quad (1)$$

$$\text{var}(\hat{d}_z) = (C(d_z + 1) - (d_z + 1)^2)/N. \quad (2)$$

The covariance between s_y and s_z in a single trial will be $\text{cov}(s_y, s_z) = E[s_y s_z] - E[s_y]E[s_z] = (d_y + 1)(d_z + 1)/C^2$, with a covariance in the entire density test, composed of N independent trials, of $(d_y + 1)(d_z + 1)N/C^2$. The covariance between \hat{d}_y and \hat{d}_z will be

$$\text{cov}(\hat{d}_y, \hat{d}_z) = C^2/N^2 \cdot \text{cov}(s_y, s_z), \quad (3)$$

$$= (d_y + 1)(d_z + 1)/N. \quad (4)$$

Fig. 1 shows overall code samples, measured DNL, and measured INL from an actual TDC. Fig. 2 shows the distribution of s_{18} and s_{70} , along with a gaussian approximation. A comparison between experimental results and the theoretical values predicted by (2) and (4) is shown in Fig. 3. To make the corresponding experimental measurements, a SPAD was coupled to the start input of a two-stage TDC whose first stage has 150 codes and ~ 20 ps resolution with a coarse second stage having a resolution of roughly ~ 3 ns. The TDC is based on the architecture presented in [3]. 400 density tests with $n = 10^5$ samples each were acquired with the SPAD at an event rate of $\lambda \approx 1$ kHz.

The variance of \hat{i}_z will be

$$\text{var}(\hat{i}_z) = \text{var}\left(\sum_{y=1}^z \hat{d}_y\right), \quad (5)$$

$$= \sum_{y=1}^z \text{var}(\hat{d}_y) + 2 \sum_{y=1}^z \sum_{x=1}^{y-1} \text{cov}(\hat{d}_x, \hat{d}_y), \quad (6)$$

$$= \frac{1}{N} \sum_{y=1}^z \left(C(d_y + 1) - (d_y + 1)^2 - 2(d_y + 1) \sum_{x=1}^{y-1} (d_x + 1) \right). \quad (7)$$

In an ideal TDC, $d_z = 0$ for all codes, and the variance in the INL measurement will reduce to

$$\text{var}(\hat{i}_z) = \frac{z \cdot (C - z)}{N}. \quad (8)$$

An intuitive explanation for the decrease to zero as $z \rightarrow c$ can be found in the situation's symmetry — the INL could just as easily be summed from the last code as the first, implying there should be no error in the last code. Fig. 5 compares this result with (7) and measurement results of the variance. There is an excellent match between the theory and the data, with the middle code showing the largest variation.

When a probabilistic exponential source is used as a uniform time interval generator, distortions to the measured INL and DNL can occur if the event rate λ of the exponential source is too high. If the exponential source is linearized, with an assumed distortion $\varepsilon/2 - \varepsilon z/c$ to the measured DNL value of code z changing from $+\varepsilon/2 = \lambda m/2$ at the TDC's initial code to $-\varepsilon/2 = -\lambda m/2$ at the TDC's final code, then the distortion to the measured INL value will be

$$\Delta \hat{i}_z = \sum_{y=0}^z (\Delta \hat{d}_y), \quad (9)$$

$$= \frac{\lambda m}{2} \left(z - \frac{z \cdot (z - 1)}{2C} \right), \quad (10)$$

which has a maximum value of roughly $\lambda m C/8$ at the TDC's middle code. This distortion was experimentally measured by artificially extending the range of the TDC using a counter to comprise the TDC's coarse portion and the previously characterized delay line to comprise the fine portion. Fig. 6 shows the measured INL value changing as a function of the non-ideal generator's event rate, with the difference plotted in Fig. 7. Because the on-FPGA temperature could not be precisely controlled, the fine delay line's LSB duration slightly shifted, which causes some differences from the expected result.

REFERENCES

[1] D. L. Snyder et al., "A mathematical model for positron-emission tomography systems having time-of-flight measurements," *Nuclear Science, IEEE Transactions on*, vol. 28, pp. 3575–3583, June 1981. [2] B. Swann et al., "A 100-ps time-resolution CMOS time-to-digital converter for positron emission tomography imaging applications," *Solid-State Circuits, IEEE Journal of*, vol. 39, pp. 1839–1852, Nov. 2004. [3] H. Menninga et al., "A multi-channel, 10ps resolution, FPGA-based TDC with 300MS/s throughput for open-source PET applications," in *Nuclear Science Symposium and Medical Imaging Conference (NSS/MIC), 2011 IEEE*, pp. 1515–1522, Oct. 2011.

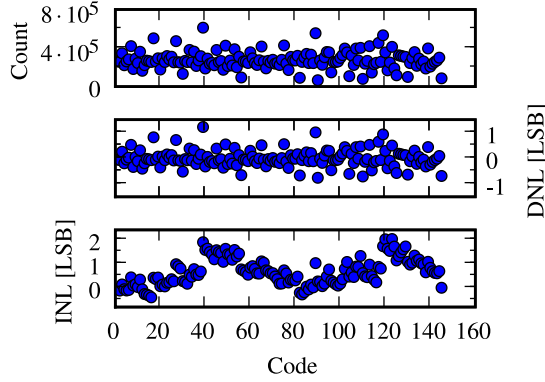


Fig. 1. Measured TDC samples, DNL, and INL vs. code — results are from 400 density tests with 100,000 samples per test

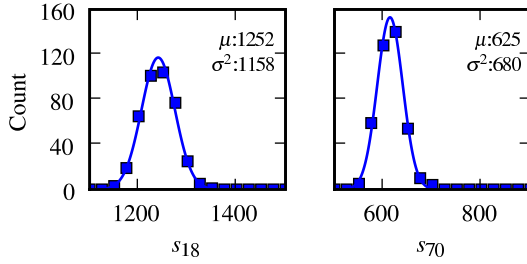


Fig. 2. s_z Histograms — shown are the experimental values (shapes) and normal distributions with a matching mean and variance (lines)

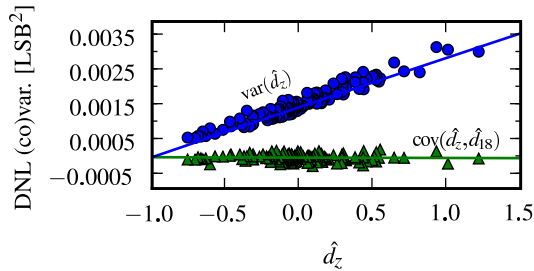


Fig. 3. $\text{var}(\hat{d}_z)$ and $\text{cov}(\hat{d}_z, \hat{d}_{70})$ vs. \hat{d}_z — shown are the experimental values (shapes) and predicted values $\text{var}(\hat{d}_z) \approx (C(\hat{d}_z + 1) - (\hat{d}_z + 1)^2)/N$ and $\text{cov}(\hat{d}_z, \hat{d}_{70}) \approx (\hat{d}_z + 1)(\hat{d}_{70} + 1)/N$

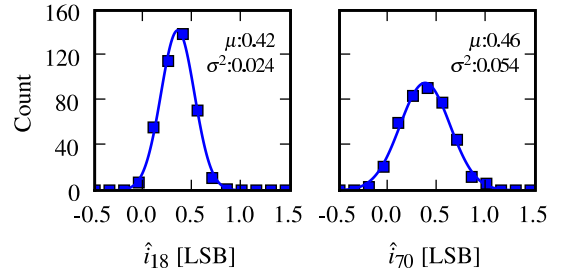


Fig. 4. \hat{i}_z Histograms — shown are experimental values (shapes) and normal distributions with a matching mean and variance (lines)

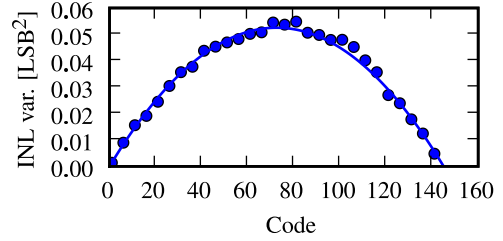


Fig. 5. $\text{var}(\hat{i}_z)$ vs. z — shown are the experimental values (shapes) and predicted value $\text{var}(\hat{i}_z) \approx z(C-z)/N$.

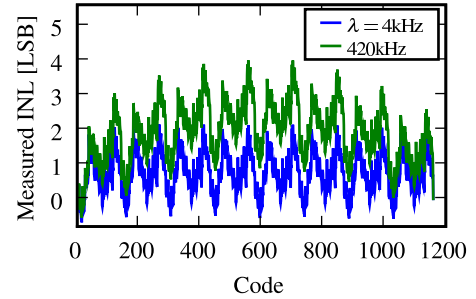


Fig. 6. \hat{i}_z vs. z for Two Different λ — eight times as many codes occur for these tests as those in Fig. 1 since the tdc range has been extended using a coarse counter. Each test has 40M samples.

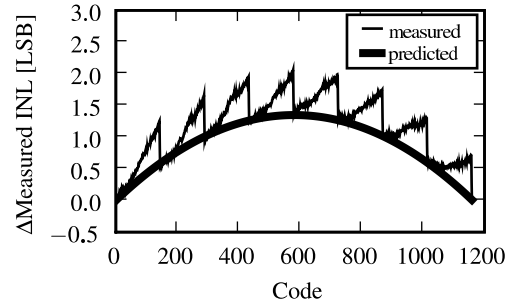


Fig. 7. $\Delta \hat{i}_z$ vs. z — the eight ramp-shaped curves are due to temperature differences, as the LSB of the fine delay line is very sensitive to temperature. Predicted values are from (10)